ChemComm

Accepted Manuscript

This article can be cited before page numbers have been issued, to do this please use: K. Liu, A. Mukhopadhyay, A. Ashcraft, C. Liu, A. Levy, P. Blackwelder and J. Olivier, *Chem. Commun.*, 2019, DOI: 10.1039/C9CC01939A.

This is an Accepted Manuscript, which has been through the Royal Society of Chemistry peer review process and has been accepted for publication.

Accepted Manuscripts are published online shortly after acceptance, before technical editing, formatting and proof reading. Using this free service, authors can make their results available to the community, in citable form, before we publish the edited article. We will replace this Accepted Manuscript with the edited and formatted Advance Article as soon as it is available.

You can find more information about Accepted Manuscripts in the author guidelines.

Please note that technical editing may introduce minor changes to the text and/or graphics, which may alter content. The journal's standard Terms & Conditions and the ethical guidelines, outlined in our author and reviewer resource centre, still apply. In no event shall the Royal Society of Chemistry be held responsible for any errors or omissions in this Accepted Manuscript or any consequences arising from the use of any information it contains.

ROYAL SOCIETY OF CHEMISTRY View Article Online
DOI: 10.1039/C9CC01939A

Journal Name

COMMUNICATION

Reconfiguration of π-Conjugated Superstructures Enabled by Redox-Assisted Assembly

Kaixuan Liu,[a] Arindam Mukhopadhyay,[a] Adam Ashcraft,[a] Chuan Liu,[a] Adam Levy,[a] Patricia Blackwelder,[b,c] and Jean-Hubert Olivier [a]*

Received 00th January 20xx,
Accepted 00th January 20xx

DOI: 10.1039/x0xx00000x

www.rsc.org/

We show that n-doping supramolecular assemblies built from perylene diimide units provides a means to modulate the structure-function properties of these materials. In addition to highlighting design principles, a combination of spectroscopic and microscopic characterization correlates an increase of free-exciton bandwidth with the formation of mesoscale hierarchical superstructures.

The development of molecular strategies to modulate structure-function relationships of nanoscale objects opens new avenues to construct organic semiconducting materials equipped with emergent (opto)electronic properties.[1-3] Contingent on the solvent dielectric property,[4] heating-cooling cycles,[5] external forces,[6] and the use of chemical fuels,[7-8] thermodynamic equilibrium, static and dissipative out-of-equilibrium states can be formed and dictate the structure-function properties of non-covalent assemblies.[9-10] At the molecular level, conformations of supramolecular polymers built from π-conjugated chromophores are regulated by non-covalent interactions between subunits that consequently regulate the extent to which frontier molecular orbitals overlap.[11] Electrostatic interaction and local electric field are two parameters that are recognized to play an important role in defining the orientation of building blocks.[12-13] Pioneering experimental and theoretical studies have unambiguously demonstrated that minor displacements between neighboring chromophores can result in a profound perturbation of the photophysical properties evidenced in superstructures.[14-15] Intricate interplays between structural parameters and electronic properties can be leveraged to modify the structure-function properties of supramolecular polymers.

Due to their unique photophysical and electrochemical properties, perylene-3,4:9,10-bis(dicarboxyimide) (PDI) derivatives have been extensively exploited as building blocks to investigate assembly processes.[16-18] Diverging from conventional heating-cooling processes recent studies have demonstrated that redox treatment of one-dimensional (1D) PDI-based supramolecular polymers can assist in navigating the assembly free-energy landscape and form kinetically trapped superstructures characterized by structure-function relationships not evidenced in initially formed, equilibrium architectures.[19-20] Aiming to further expand the scope of redox-assisted assembly and investigate the extent to which structure-function relationships of non-covalent assemblies can be modulated by design, we have synthesized the two PDI-based building blocks, **PDI-C_3Im-C_2OH** and **PDI-TEOAm-C_2OH,** presented in Scheme 1A and studied their assembly properties following the flow chart shown in Scheme 1B. While these two building blocks share similar structural attributes as both are flanked with cationic functional groups (imidazolium or ammonium) and terminal hydroxyl functions, linear linkers that tether redox active, hydrophobic PDI cores and hydrophilic functionalities have been modified. As

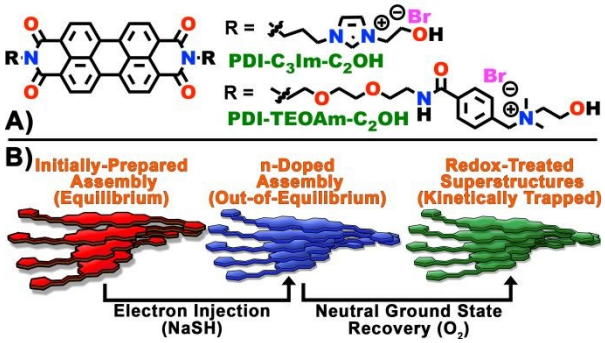

Scheme 1: (A) Molecular Structures of the amphiphilic PDI-based building blocks utilized to investigate redox-assisted assembly process shown in (B).

[a] *Department of Chemistry, University of Miami, Cox Science Center, 1301 Memorial Drive, Coral Gables, FL 33146*
jh.olivier@miami.edu
[b] Center for Advanced Microscopy (UMCAM), Department of Chemistry, University of Miami, Coral Gables, FL 33146
[c] Marine Geological Sciences, Rosentsteil School of Marine and Atmospheric Science, University of Miami, 4600 Rickenbacker Causeway, Miami, FL 33149

Electronic Supplementary Information (ESI) available: Synthesis, characterization and aggregation mechanisms of redox-active building blocks. SEM, TEM, absorption spectra, NMR, IR, MS, See DOI: xxxxxxxxxxxxxxxxxx

View Article Online DOI: 10.1039/C9CC01939A

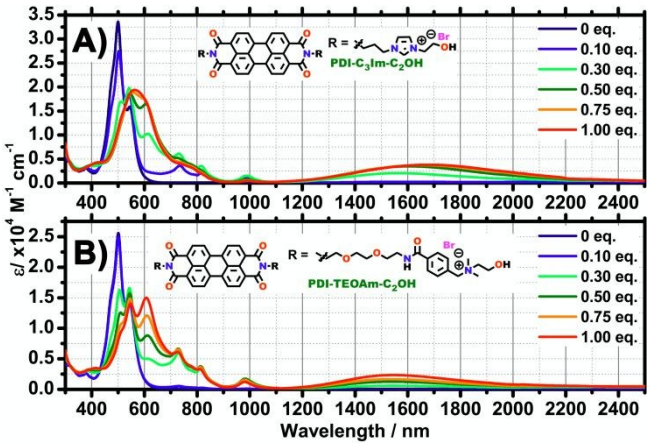

Fig. 1: Ground-state electronic absorption spectra recorded in D_2O for non-covalent **PDI-C_3Im-C_2OH (A)** and **PDI-TEOAm-C_2OH (B)** assemblies upon the addition of sodium hydrosulfide (NaSH). Experimental conditions: initial [PDI]= 200 μM; final [PDI] = 140 μM; T = 20 ˚C; Argon atmosphere, optical pathlength = 2 mm; initial pH = 7.00; final pH = 10.85; initial ionic strength = 4.22 x 10^{-4} M; final ionic strength = 2.53 x 10^{-4} M.

chronicled in Figure S1-S4 and associated text, temperature-dependent aggregation experiments performed with **PDI-C_3Im-C_2OH** and **PDI-TEOAm-C_2OH** building blocks in water and under identical concentration conditions (5 μM) suggest that the combination of propylene linker and imidazolium cation facilitates a more complete supramolecular polymerization process compared to that of ethoxyether tether (TEO) and ammonium cation.

To glean further insights into the structure-function relationships of the supramolecular polymers built from **PDI-C_3Im-C_2OH** and **PDI-TEOAm-C_2OH** subunits, reductive titrations have been conducted and the results are chronicled in Fig. 1. Because electronic properties of organic superstructures and aggregates are intimately related to the conformation of building blocks,[21] we hypothesized that spectroscopic signatures of n-doped PDI-assembly (Scheme 1B) can be exploited as a sensitive diagnostic tool to probe any potential perturbation of assembly conformation. As evidenced in Fig. 1A, implementation of a **PDI-C_3Im-C_2OH** D_2O solution with sodium hydrosulfide (NaSH) utilized as a chemical reductant is accompanied with the apparition of absorptive features that span the visible to near infrared (NIR) detection windows and indicate the formation of n-doped PDI assembly. For further details on the reductive titration experiments please refer to Section 4 in the ESI. It is interesting to underscore that at earlier titration points (0.1 to 0.3 eq.), the spectroscopic signatures of aggregated PDI-radical anion can be detected at 988, 816, 731, and 615 nm,[22] while further addition of reductant (0.5 eq. to 1.0 eq.) witnesses the formation of a new species confirmed by: 1) the formation of broad, asymmetric absorption bands between 400 and 900 nm, 2) the drastic decrease of the 988-nm band diagnostic of aggregated PDI-radical anion, and 3) the bathochromic shift by more than 130 nm (60 meV) of the broad NIR transition initially centered at 1570 nm. Notably, increasing the concentration of reductant above 1 eq. is not associated with any relevant spectroscopic change as shown in Figure S6. Congruent with the fact that previous studies have

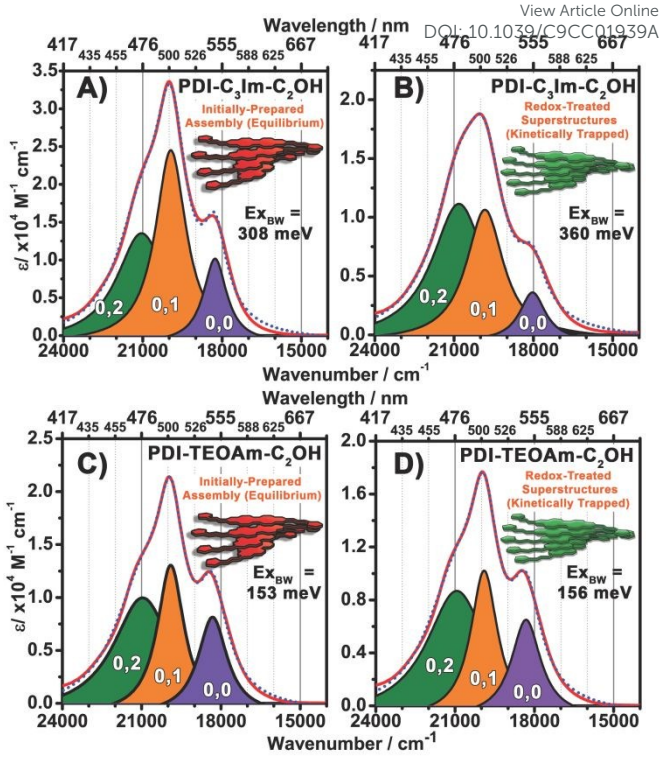

Fig. 2: Deconvolution of the experimental ground state electronic absorption spectra (red) recorded for **PDI-C_3Im-C_2OH** (A-B) and **PDI-TEOAm-C_2OH** (C-D) before and after redox-assisted assembly respectively. The deconvoluted purple, orange and green peaks correspond to 0-0, 0-1, 0-2 vibronic transitions. The reconvoluted absorption spectra are shown by the dotted blue lines.

attributed the emergence of NIR spectral signatures with the formation of π-anion stacks,[23-26] we posit that electron injection into **PDI-C_3Im-C_2OH** assembly initiates the formation of a n-doped assembly that does not share the same electronic properties as the aggregated PDI-radical anion.

In sharp contrast, the **PDI-TEOAm-C_2OH** reductive titration experiments chronicled in Fig. 1B preserve the spectroscopic signatures reminiscent to that of aggregated PDI-radical anion.[22] This conclusion is based on the fact that addition of up to 5 eq. of sodium hydrosulfide is characterized by: 1) the continuous rise of an absorption band at 608 nm, and 2) the lack of discernible shift of the 1550 nm absorption band as a function of reductant equivalent (Figure S7). Furthermore, it is important to emphasize the 135 nm (70 meV) shift when comparing the NIR absorptive features of the **PDI-TEOAm-C_2OH** (1550 nm) and n-doped **PDI-C_3Im-C_2OH** (1700 nm) assembly. All taken together, these reductive titration experiments underscore that n-doped **PDI-C_3Im-C_2OH** superstructure is characterized by electronic states that differ with respect to those evidenced in n-doped **PDI-TEOAm-C_2OH** assembly.

To further investigate if n-doped assemblies can be exploited to navigate the assembly free-energy landscapes and modify the structure-function properties of equilibrium assemblies, Fig. 2 compares the ground state electronic absorption spectra (EAS) of oxygen-neutralized assemblies with those of initially formed supramolecular polymers (Scheme 1B). Please note that the

kinetically trapped assembly was formed by letting the freshly oxidized n-doped assemblies age during 18 hours. Deconvolution of

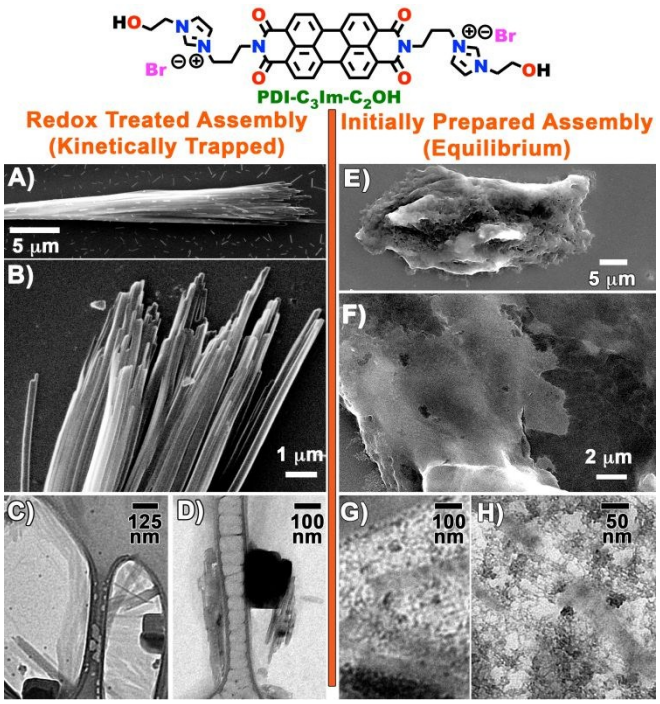

Fig. 3: Microscopic characterization of kinetically trapped (A-D) and equilibrium (E-H) **PDI-C_3Im-C_2OH** assemblies from a D_2O solution. Comparative scanning electron microscopic (SEM) images recorded after (A-B) and before redox treatment (E-F) highlight the formation of hierarchical mesoscale materials during redox-assisted assembly process. Transmission electron microscopic (TEM) images acquired after (C-D) and before redox treatment (G-H) show a drastic change of superstructure morphology at the nanoscale.

the EAS of **PDI-TEOAm-C_2OH** and **PDI-C_3Im-C_2OH** before and after titration allows for calculation of the oscillator strength of the 0-0, 0-1, and 0-2 vibronic transitions between the PDI relaxed ground-state S_0 and the first singlet excited state S_1. Analysis of the deconvoluted **PDI-C_3Im-C_2OH** EAS indicates a non-negligible redistribution of the 0-0 and 0-1 transition oscillator strengths suggesting that n-doping the **PDI-C_3Im-C_2OH** superstructure perturbs the photophysical properties of the initially formed assembly. In sharp contrast, no apparent evolution of the photophysical properties is evidenced when comparing the oscillator strength of the 0-0 and 0-1 transitions in **PDI-TEOAm-C_2OH** assemblies before and after the n-doping process.

Seminal studies have demonstrated that Ex_{BW} of π-conjugated superstructures that feature PDI-based building blocks and other π-conjugated units is intimately related to frontier molecular orbital overlaps. Consequently, Ex_{BW} can be utilized to glean additional information on structure-function relationships of non-covalent assemblies.[15, 27-28] Using the model pioneered by Spano *et al.* (see Section 5 in ESI), we have calculated the Ex_{BW} for **PDI-C_3Im-C_2OH** assemblies before and after the n-doping process and compared it to that of **PDI-TEOAm-C_2OH** assemblies (Table 1). As suggested by the change of oscillator strength initially detected in the **PDI-C_3Im-C_2OH** superstructure, an increase of more than 52 meV is evidenced when comparing the initially formed assembly (Ex_{BW} = 308 meV) and redox-treated assembly (Ex_{BW} = 360 meV). In sharp contrast, n-doping the initially formed **PDI-TEOAm-C_2OH** assembly does not increase the Ex_{BW} as the calculated Ex_{BW} before (153 meV) and after redox treatment **PDI-TEOAm-C_2OH** (156 meV) remains virtually unaltered (Table 1). Please note that to ensure that the reported change of electronic properties is not a consequence of ionic strength perturbation achieved during the reductive titration experiment, the Ex_{BW} for each initially formed assembly has been calculated from the EAS of a solution that mimics the ionic strength of the solution after reductive titration (see control samples, Section 4 in the ESI). By combining reductive titration experiments with the photophysical properties of **PDI-C_3Im-C_2OH** and **PDI-TEOAm-C_2OH** assemblies before and after redox treatment, the apparent increase of Ex_{BW} evidenced in the redox-treated **PDI-C_3Im-C_2OH** superstructure can be associated with the n-doped intermediate assembly formed during reductive titration experiments. This correlation is based on the fact that, when compared to **PDI-TEOAm-C_2OH**, the red-shifted NIR spectroscopic signatures of the n-doped **PDI-C_3Im-C_2OH** intermediate at 1700 nm may indicate a higher magnitude of π-orbital interactions.

Because perturbation of the photophysical properties of π-conjugated superstructures can originate from a structural reconfiguration, we have investigated the solid-state morphologies of **PDI-C_3Im-C_2OH** superstructure before and after redox treatment (Fig. 3 and Fig. S8-S17) and compared it to that evidenced by **PDI-TEOAm-C_2OH** assembly (Fig. S18-S22). Comparing SEM images recorded for initially prepared **PDI-C_3Im-C_2OH** assembly (Fig. 3E-F) with that corresponding to redox-treated superstructures (Fig. 3A-B) reveals a striking contrast. While drop casting the initially prepared assembly engenders the formation of aggregates that appear amorphous under SEM, redox-treated superstructures organize into 1D materials spanning the microscale dimension as seen in Fig. 3A. It is interesting to note that rod-like structures with a width of 140 to 170 nm laterally interact to evolve into compact, micron-sized fiber-like materials. Noteworthy is the fact that the hierarchical mesoscale objects presented in Fig. 3A-B are in all likelihood tracing their genesis from local concentration effects associated with the drop casting deposition method and suggest non-negligible perturbation of the solvated **PDI-C_3Im-C_2OH** superstructure conformation with respect to that of the initially prepared, parent assemblies. To gain further insights into the nanoscale superstructure comprising fiber-like materials, we monitored redox-treated **PDI-C_3Im-C_2OH** superstructures and precursor assemblies by TEM. As can be seen in Fig. 3C-D, rod-like structures sharing a 15-40 nm width are easily detectable and further confirm our initial hypothesis that redox-assisted assembly enforces formation of mesoscale hierarchical superstructures. Sharply contrasting this finding, TEM images recorded for parent **PDI-C_3Im-C_2OH** assembly fail to demonstrate any organized domains as shown in Fig. 3G-H.

By combining the data presented so far for **PDI-C_3Im-C_2OH**-derived supramolecular architectures, the increase of Ex_{BW} can be associated with the formation of hierarchical materials. This

assumption is further validated by elucidating the solid-state morphologies of **PDI-TEOAm-C_2OH**-derived assemblies. As expected from the lack of Ex_{BW} increase reported for redox-treated **PDI-TEOAm-C_2OH** assembly, no distinguishable organized domains are observed in the SEM images shown in Fig. S18-S22 where globular, amorphous aggregates best characterize the solid-state morphology of this class of assembly.

Comparing the photophysical properties and solid-state morphologies presented for **PDI-C_3Im-C_2OH** superstructure with those of **PDI-TEOAm-C_2OH** assembly allows the elucidation of critical parameters that need to be considered during a redox-assisted assembly process. As indicated by the temperature-dependent aggregation and the reductive titration experiments, TEO side chains flanked on PDI cores confers hydrophilicity to **PDI-TEOAm-C_2OH** building blocks that prevent access to superstructure conformation, during the n-doping process, comparable to that of **PDI-C_3Im-C_2OH**. Consequently, while recovery of the neutral ground state of the **PDI-C_3Im-C_2OH** n-doped intermediate is accompanied by an increase of Ex_{BW}, no apparent change of photophysical properties is evidenced in redox-treated **PDI-TEOAm-C_2OH** assembly. This observation underscores the pivotal role played by the n-doped intermediates. We postulate that upon electron injection, electrostatic repulsion between negatively charged **PDI-TEOAm-C_2OH** hydrophilic building blocks may compromise the assembly integrity. Furthermore, the suspected conformational change of the **PDI-C_3Im-C_2OH** superstructure, signaled by the increase of Ex_{BW}, is further validated by the formation of mesoscale 1D hierarchical materials.

In conclusion, we have demonstrated that the initial photophysical and solid-state properties of PDI-derived supramolecular polymers can be modified by exploiting redox-assisted assembly. Analysis of the reductive titration, Ex_{BW}, and morphological attributes of **PDI-C_3Im-C_2OH** and **PDI-TEOAm-C_2OH** assemblies before and after redox treatment has unraveled pivotal structural and electronic parameters that enable the evolution of structure-function relationships. Because reductive titrations of initially prepared **PDI-C_3Im-C_2OH** assemblies demonstrate a 70-meV bathochromic shift of the π-anion stack spectral signature when compared to that of **PDI-TEOAm-C_2OH** assemblies, the increase of Ex_{BW}, exclusively evidenced in **PDI-C_3Im-C_2OH** superstructures, can be correlated to the electronic properties of the n-doped intermediates. To complement the change of electronic function, redox-assisted assembly of the **PDI-C_3Im-C_2OH** supramolecular polymer enforces the formation of highly ordered 1D mesoscale materials that span the nano-to-microscale dimensions. We postulate that n-doping the initially prepared **PDI-C_3Im-C_2OH** assembly engenders a superstructure conformational change that assists the formation of hierarchical supramolecular architectures. This work provides a new tool to navigate the self-assembly free energy landscape and create semiconducting superstructures relevant to optoelectronic applications.

This work was supported by the University of Miami. Additional support provided by the Arnold and Mabel Beckman Foundation (BYI Award 2018) is gratefully acknowledged. We thank Brianna Bernard and Victor Paulino for their constructive comments.

Conflicts of interest

View Article Online
DOI: 10.1039/C9CC01939A

There are no conflicts to declare.

Notes and references

1.Moulin, E.; Niess, F.; Maaloum, M.; Buhler, E.; Nyrkova, I.; Giuseppone, N. *Angew. Chem. Int. Ed.* **2010**, *49*, 6974-6978.
2.van der Weegen, R.; Teunissen Abraham, J. P.; Meijer, E. W. *Chem. Eur. J.* **2017**, *23*, 3773-3783.
3.Liu, C.; Liu, K.; Klütke, J.; Ashcraft, A.; Steefel, S.; Olivier, J.-H. *J. Mater. Chem. C* **2018**, *6*, 11980-11991.
4.Mabesoone, M. F. J.; Markvoort, A. J.; Banno, M.; Yamaguchi, T.; Helmich, F.; Naito, Y.; Yashima, E.; Palmans, A. R. A.; Meijer, E. W. *J. Am. Chem. Soc.* **2018**, *140*, 7810-7819.
5.Fukui, T.; Kawai, S.; Fujinuma, S.; Matsushita, Y.; Yasuda, T.; Sakurai, T.; Seki, S.; Takeuchi, M.; Sugiyasu, K. *Nat. Chem.* **2016**, *9*, 493.
6.Micali, N.; Engelkamp, H.; van Rhee, P. G.; Christianen, P. C. M.; Scolaro, L. M.; Maan, J. C. *Nat. Chem.* **2012**, *4*, 201.
7.Dhiman, S.; Jain, A.; George, S. J. *Angew. Chem. Int. Ed.* **2017**, *56*, 1329-1333.
8.Dhiman, S.; Sarkar, A.; George, S. J. *RSC Advances* **2018**, *8*, 18913-18925.
9.De Greef, T. F. A.; Smulders, M. M. J.; Wolffs, M.; Schenning, A. P. H. J.; Sijbesma, R. P.; Meijer, E. W. *Chem. Rev.* **2009**, *109*, 5687-5754.
10.Korevaar, P. A.; de Greef, T. F. A.; Meijer, E. W. *Chem. Mater.* **2014**, *26*, 576-586.
11.Ostroverkhova, O. *Chem. Rev.* **2016**, *116*, 13279-13412.
12.Martinez, C. R.; Iverson, B. L. *Chem. Sci.* **2012**, *3*, 2191-2201.
13.Raju, R. K.; Bloom, J. W. G.; Wheeler, S. E. *J. Chem. Theory Comput.* **2013**, *9*, 3479-3490.
14.Kaufmann, C.; Bialas, D.; Stolte, M.; Würthner, F. *J. Am. Chem. Soc.* **2018**, *140*, 9986-9995.
15.Hestand, N. J.; Spano, F. C. *Acc. Chem. Res.* **2017**, *50*, 341-350.
16.Görl, D.; Zhang, X.; Würthner, F. *Angew. Chem. Int. Ed.* **2012**, *51*, 6328-6348.
17.Sorrenti, A.; Leira-Iglesias, J.; Sato, A.; Hermans, T. M. *Nat. Commun.* **2017**, *8*, 15899.
18.Leira-Iglesias, J.; Tassoni, A.; Adachi, T.; Stich, M.; Hermans, T. M. *Nat. Nanotechnol.* **2018**, *13*, 1021-1027.
19.Liu, K.; Levy, A.; Liu, C.; Olivier, J.-H. *Chem. Mater.* **2018**, *30*, 2143-2150.
20.Leira-Iglesias, J.; Sorrenti, A.; Sato, A.; Dunne, P. A.; Hermans, T. M. *Chem. Commun.* **2016**, *52*, 9009-9012.
21.Vura-Weis, J.; Ratner, M. A.; Wasielewski, M. R. *J. Am. Chem. Soc.* **2010**, *132*, 1738-1739.
22.Marcon, R. O.; Brochsztain, S. *J. Phys. Chem. A* **2009**, *113*, 1747-1752.
23.Graf, D. D.; Duan, R. G.; Campbell, J. P.; Miller, L. L.; Mann, K. R. *J. Am. Chem. Soc.* **1997**, *119*, 5888-5899.
24.Miller, L. L.; Mann, K. R. *Acc. Chem. Res.* **1996**, *29*, 417-423.
25.Zhong, C. J.; Kwan, W. S. V.; Miller, L. L. *Chem. Mater.* **1992**, *4*, 1423-1428.
26.Wu, Y.; Frasconi, M.; Gardner, D. M.; McGonigal, P. R.; Schneebeli, S. T.; Wasielewski, M. R.; Stoddart, J. F. *Angew. Chem. Int. Ed.* **2014**, *53*, 9476-9481.
27.Spano, F. C.; Silva, C. *Annu. Rev. Phys. Chem.* **2014**, *65*, 477-500.
28.Clark, J.; Chang, J.-F.; Spano, F. C.; Friend, R. H.; Silva, C. *Appl. Phys. Lett.* **2009**, *94*, 163306.

View Article Online
DOI: 10.1039/C9CC01939A

TOC

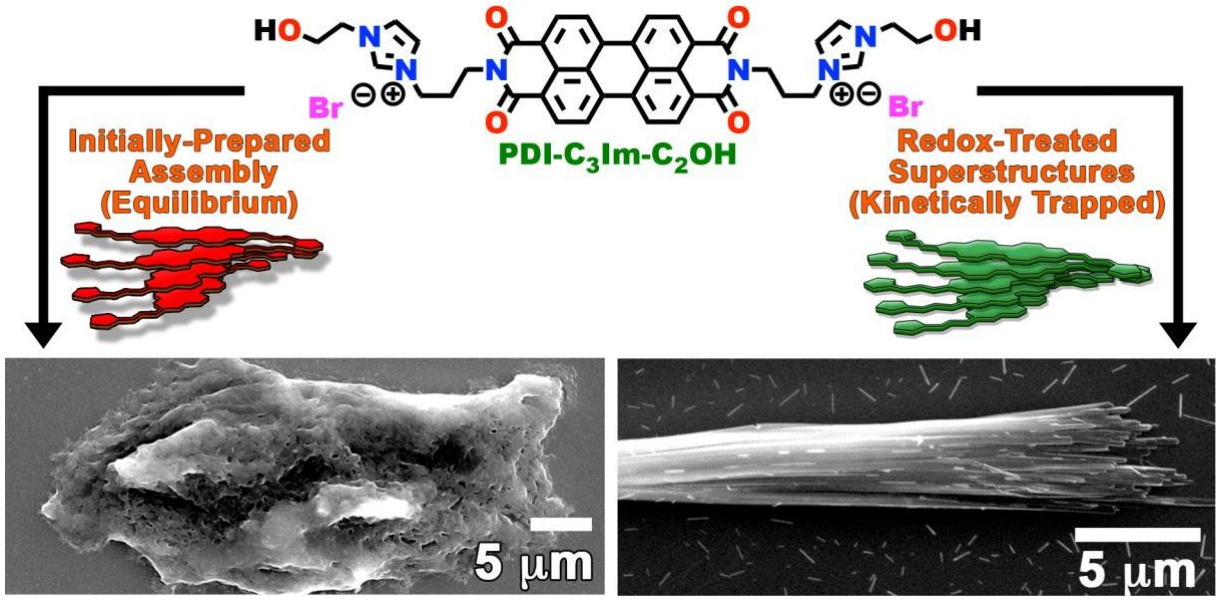

Redox-Assisted Assembly enforces reconfiguration of π-conjugated superstructures